Laser annealing of silicon

V P GODBOLE and S M CHAUDHARI

Department of Physics, University of Poona, Pune 411 007, India

Abstract. In recent years laser processing has attracted much attention in view of its potential use in basic solid-state and material science research as well as in new processing technologies. The dominant feature of laser processing being the deposition of large amounts of energy (a few J/cm^2) over very short time scales (a few tens of nanoseconds), it leads to melting of surface layers of solid followed by rapid resolidification. In this article, a few basic consequences of such laser-induced phenomena in silicon are reviewed.

Keywords. Laser annealing; silicon.

The term "laser annealing" was born after initial studies (Gerasimenko *et al* 1975) in which it was observed that structural damage produced in ion-implanted c-Si can be removed and electrical activation of doped layers can be increased by using pulsed laser irradiation. After the initial establishment of this phenomenon, an extensive amount of research work has been and is being carried out. These studies have revealed more interesting features of the process and thus the term laser annealing is nowadays used for a much broader class of phenomena ranging from laser-induced growth to alloying.

In all these studies two types of laser systems have been utilized, viz. (i) continuous wave (CW) lasers such as Ar^+ and CO_2^+ lasers and (ii) pulsed lasers such as ruby and Nd–YAG lasers. Pulsed lasers can be divided into three types, viz. pulsed free running lasers with pulse duration of a few milliseconds, Q-switched lasers with pulse-width of mostly 20–50 nanoseconds, and mode-locked lasers with pulse duration of a few picoseconds. In a typical CW laser annealing experiment, the laser beam is focused to a suitable size and then scanned all over the substrate area. In the case of pulsed laser annealing the available beam size is sufficiently large and has high power density so that processing can be done in a single laser shot, although in some cases it can also be operated in the focusing-scanning mode. The energies used are generally of the order of 1 J/cm^2 in the case of pulsed laser annealing and a few tens of watts in CW laser annealing for the case of silicon.

Soon after the demonstration of laser annealing in ion-implanted silicon other semiconductor materials as well as disordered materials such as a-Si layers produced by methods other than ion implantation also came under study and revealed many interesting features of laser processing. These include redistribution of implanted profiles, trapping of unusually large concentrations of dopants, epitaxial regrowth of a-Si, alloying of layers of component materials, synthesis of glassy structures at high laser energy densities, etc. Apart from these investigations there has also been, with the advent of laser-induced chemistry, a considerable interest in recent years to explore the use of lasers in all phases of the processing of semiconductor devices. Lasers have facilitated production of submicrometre features without the aid of chemical lithography. In this article, however, we will be mainly concerned with the laser-induced phenomena pertaining to annealing effects in silicon.

After the initial demonstration of laser annealing in silicon, scientists working in the field focused their attention on the basic question of what physical mechanisms are responsible for laser-induced annealing, particularly the issue of the nature of energy transfer from laser to material. Based on some preliminary studies on heat flow calculations it was suggested that laser annealing is a consequence of melting of surface layers followed by liquid phase epitaxy during cool-down of the molten layer. In these studies it was believed that an electron–hole plasma is produced upon absorption of laser energy, which is then instantaneously transferred to the phonon system of the crystal lattice of the solid material, leading to melting. The transformations take place during molten state of solid as well as during rapid regrowth of material. Extensive theoretical investigations have been carried out (Baeri *et al* 1979; Bhattacharyya *et al* 1981; Wood *et al* 1981; Cole *et al* 1984) to study the dynamics of melting and resolidification of amorphous silicon layers. Figure 1a shows the typical temperature–time profiles at several depths inside the amorphous silicon layer while time evolution of the solid–liquid interface for different power densities is shown in figure 1b. Although this so-called thermal model was becoming widely acceptable, a number of publications appeared, exploring the validity of this model. In fact the Russians stressed, right from the beginning, that the annealing is a consequence of non-thermal effects. It was argued that the primary channel of absorption of laser energy is excitation of the electronic system, leading to the formation of a dense electron–hole plasma which takes up a greater portion of the laser energy. Laser photons of energy greater than that of the band gap generate electron–hole pairs. Free electrons and holes may also absorb energy from photons and be promoted to states of higher kinetic energy in the conduction and valence bands. In all cases, the input energy flows into electronic excitation of the solid. The central issue was the rate at which the energy moves from electrons to phonons, thus becoming heat. If transfer is sufficiently fast compared to the duration of excitation (length of laser pulse), the electronic system will never be far from equilibrium with the lattice; if it is slow, electrons may become much hotter than the lattice. It was suggested that many results of laser annealing could be due to the effect of this "hot plasma" on atomic rearrangements in the solid. The issue of energy transfer was thus controversial for a long time. On the one hand there appeared some theoretical calculations and also some experimental evidence
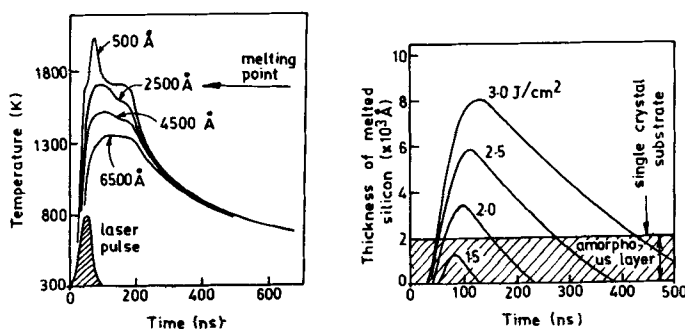

Figure 1. (a) Temperature-time profiles at several depths inside the amorphous silicon layer. The energy density of the Gaussian laser pulse was 1·5 J/cm². (b) Time evolution of the solid-liquid interface for 2000 Å-thick amorphous silicon layer on a single crystal substrate for different energy densities of the laser pulse (50 ns) (Baeri *et al* 1979).

supporting strictly the thermal model; on the other hand there were some other reports that ruled out the thermal model in favour of the "hot plasma" model. Extensive investigations have been carried out to resolve this issue. These basically include experiments to study redistribution and segregation of implanted impurities as a result of laser annealing, the phenomenon of epitaxial growth of amorphous structures, time-dependent reflection and transmission measurements during and following an excitation pulse, time-dependent electrical resistivity measurement, measurement of velocity distribution of evaporated atoms and thermionic electron emission, time-dependent X-ray Bragg scattering and Raman scattering, etc. In the following paragraphs we have briefly reviewed some of these experimental results.

A number of experimental observations have been made on redistribution and segregation of implanted dopants in crystalline silicon after pulsed laser annealing, and these are remarkably well explained by the model that simply involves heat, viz. excitation of the phonon system and not the electronic system. Experiments carried out by Baeri *et al* (1978) revealed strong surface segregation of implanted Cu in silicon; similar results were obtained (White *et al* 1978) in the case of other transition dopants such as Fe and Zn. In some studies results were correlated in a rather simple way with the thermal model. The key factor for expecting such a correlation was basically the assumption that given the freezing rate the nature of redistribution should bear some relationship with the known values of diffusivity and equilibrium distribution coefficient of dopant in molten silicon. However, no such concrete correlation was observed in other studies. Hoonhout *et al* (1979) carried out some systematic studies on redistribution of Ga, Ge, Sn, As, Sb, Bi, Se and Te dopants and found that the nature of redistribution depends upon the type of impurity (figure 2). In some cases broadening of implanted profile was observed while in some other cases strong segregation effects were seen. The variation of segregation coefficient of Bi and In in Si are measured (Baeri *et al* 1981; Poate 1982) as a function of interface velocity for ⟨111⟩ and ⟨100⟩ oriented crystals (figure 3). In these studies surface layers were melted by ruby laser irradiation and liquid–solid interface velocities during regrowth were varied from 1 to 7 m/sec by changing the laser pulse length. It was observed that segregation coefficients are strongly dependent on interface velocity and orientation of crystal. The experiments of White *et al* (1980) on group III and group V type dopants in silicon revealed that substitutionality occurs after laser annealing at concentrations far in excess of equilibrium solid solubilities (figure 4). An investigation of the physical basis for such a supersaturation has been carried out by Poate and Brown (1982). These authors modelled the trapping effects in terms of competition between the speed of
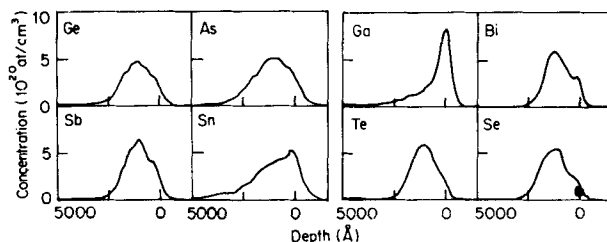
Figure 2. Measured depth profiles of dopant atoms after ruby laser annealing at approximately $1.6 \, \text{J/cm}^2$ as obtained from the random backscattering spectra without correcting for detector resolution (Hoonhout *et al* 1979).
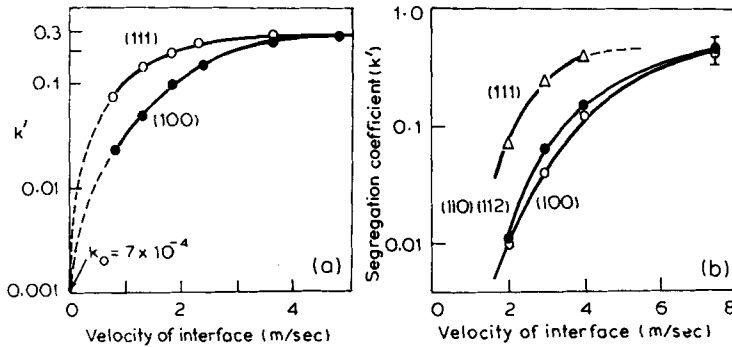
Figure 3. Variation of segregation coefficient as a function of interface velocity and $\langle 100 \rangle$ and $\langle 111 \rangle$ orientation. **(a)** Bi in Si (Baeri *et al* 1981); **(b)** In in Si (Poate *et al* 1982).
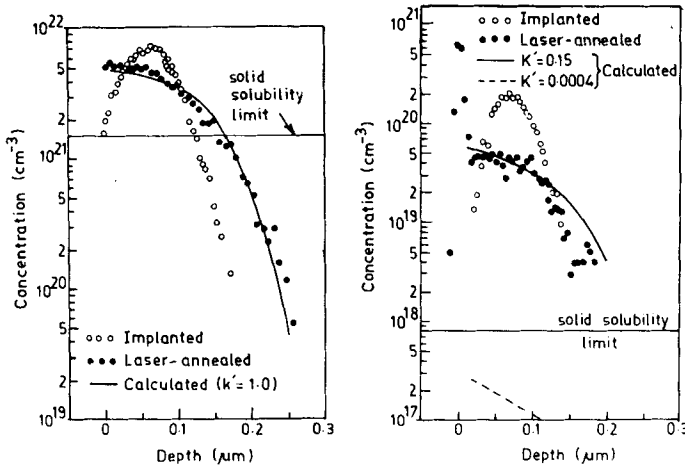

Figure 4. The comparison of experimental and calculated dopant profiles in silicon. **(a)** For As: 100 keV, $6\cdot4 \times 10^{16}$ ions/cm^2; **(b)** for In: 125 keV, $1\cdot2 \times 10^{15}$ ions/cm^2 (White *et al* 1980).

the moving liquid–solid interface and diffusion of impurities away from the interface. Cahn *et al* (1980) considered thermodynamic limits for the maximum amount of impurity that silicon can incorporate. Based on these calculations Narayan (1981) observed that the high concentration of dopants segregating ahead of the interface lower the melting point, and an instability, known as "constitutional supercooling", develops. This phenomenon leads to lateral segregation and results in the formation of cellular structure. Prussin and Van der Ohe (1980) have discussed the mechanism of pulsed laser annealing of low dose ion-implanted silicon which is non-amorphous. They claim that energy release in the interaction of pulsed ruby laser with crystalline surface containing discrete implant defects occurs primarily at the defects, creating a localized hot spot leading to dissolution of defect and "heating and electrical activation" of the region adjacent to the defect.

Some systematic investigations of threshold energy density for recrystallization of ion-implanted silicon have been carried out by Tamminga *et al* (1979) and Hoonhout *et al* (1980). In these studies any correlation of threshold energy as a function of type and dose of implanted impurity, laser wavelength, thickness of

disordered layers (energy of ion-implantation), etc. was explored. The recrystallization of ion-implanted silicon as a function of irradiated energy density from laser is illustrated in figure 5. Si $\langle 100 \rangle$ was implanted with 175 keV Ge$^+$ ions at a dose of 10^{16} ions/cm^2 to induce amorphization in silicon up to a depth of 115 nm. In figure 5 RBS channeling yield along (100) axis, which is a measure of disorder, is shown. It is clearly observed that with increase in laser energy density backscattered yield decreases systematically indicating re-storage of crystallinity. Similar results have been observed in many other studies involving different types of impurities. It is clear that, typically, an energy density of 1·5 J/cm^2 is required to anneal a few hundreds of Angstroms of a-Si. Very little dependence of impurity on laser threshold energy density was observed. Figure 6 shows variation of channeling yield with respect to laser energy density for various types of dopants. In the case of As$^+$-implanted silicon threshold laser energy was found to be directly proportional to the thickness of the amorphous layer over the range 60–300 nm. The influence of temperature during ion implantation was not much, but the threshold energy was found to be sensitive to crystal orientation. Figure 7 shows backscattering spectra for $\langle 100 \rangle$ and $\langle 111 \rangle$ oriented silicon implanted with Si before and after laser annealing. It is clearly observed that annealing is efficient for $\langle 100 \rangle$ silicon. All these results indicate that laser annealing proceeds via a phase transition induced in all of disordered surface layer followed by epitaxial regrowth. The latter phase could be either thermal melt or a phase with different binding and transport properties owing to persistence of laser-induced dense electron–hole plasma. Although the results may be explained qualitatively by a strictly thermal model, no concrete evidence for this was obtained. A quantitative description of the pulsed laser annealing process would require a better knowledge of parameters such as
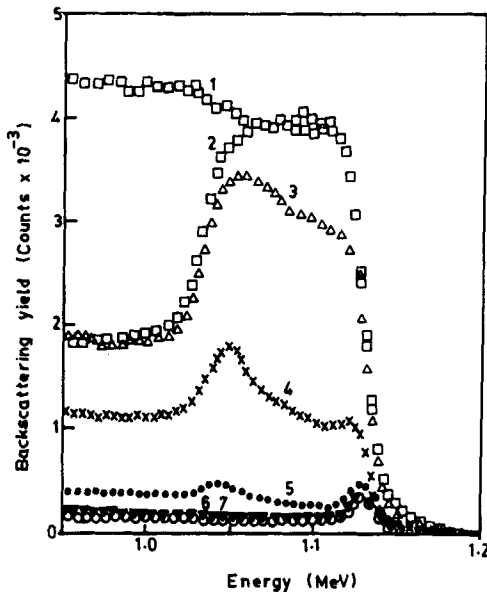

Figure 5. Backscattering spectra for Si $\langle 100 \rangle$ implanted with 175 keV, 10^{16} at/cm^2 Ge, before and after laser annealing. 1, random spectrum; 2–7, channeling spectra for the following laser treatments; 2, as implanted; 3, 0·70 J/cm^2; 4, 1·10 J/cm^2; 5, 1·35 J/cm^2; 6, 1·50 J/cm^2; 7, 1·90 J/cm^2 (Hoonhout 1981).

absorption coefficient, carrier diffusivity, phonon emission rates, etc. which was lacking during the above studies.

Apart from the types of experiments mentioned above, some other experiments have also been carried out in an effort to shed some light on laser-induced processes. For example, Galvin *et al* (1982) carried out real-time resistivity measurement to infer interface velocity during regrowth. Since the conductivity of molten silicon is much greater than that of solid silicon, it was possible, by monitoring conductivity of the sample, to determine the position of the liquid–solid interface as a function of time. The measured interface velocity of 2·8 m/sec was in agreement with the calculated value of 2·7 m/sec. Such experimental measurements provide the means to find melting and freezing rates and to subsequently infer solute trapping effects which are the most striking manifestation of rapidly moving liquid–solid interface. Liu *et al* (1982) have carried out reflectivity and thermionic electron emission measurements and observed that energy conversion time in the case of silicon is 10 picoseconds. Bhattacharyya *et al* (1981) have also carried out
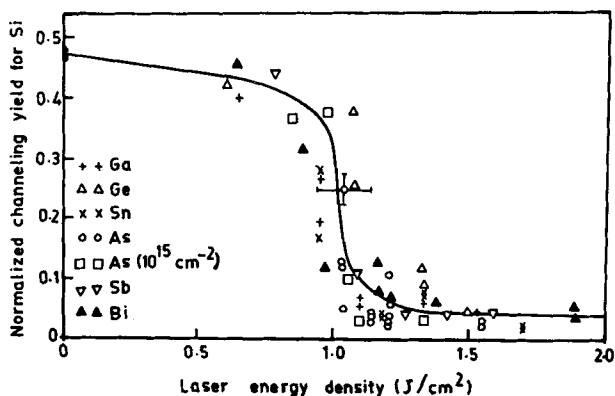

Figure 6. The channeling yield just below the disordered region normalized against the random yield as a function of energy density for Si ⟨100⟩ implanted with the elements indicated. The implantations resulted in a disordered layer with a thickness of 210 nm. (Hoonhout 1981.)
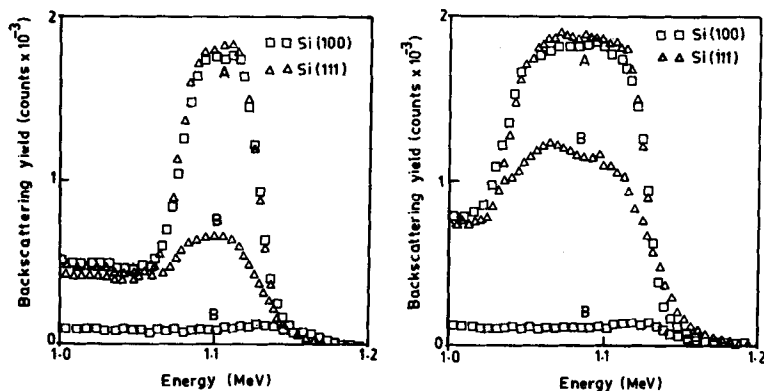

Figure 7. Backscattering spectra for Si ⟨100⟩ and Si ⟨111⟩ implanted with Si. (a) 40 keV, $5 \times 10^{15}/cm^2$; (b) 75 keV, $10^{16}/cm^2$. Curve A, as implanted; curves B, after laser annealing. (Hoonhout 1981.)

time-resolved reflectivity measurements during laser annealing of silicon. Figure 8 shows the experimental set-up as well as the results of their experiment. A typical reflectivity change at the surface during 2 J/cm² Nd–glass laser pulse is shown in figure 8b. The reflectivity increases abruptly from its value for a-Si at room temperature as the surface becomes hot. As the laser pulse nears its peak the front surface melts and reflectivity rises to a value of 65% which is consistent with the value of reflectivity for liquid silicon at 633 nm (probe laser beam). The reflectivity then stays at this value for about 200 ns and then decreases to a value corresponding to crystalline silicon at room temperature. The drop in the initial rise in reflectivity is attributed to the change in optical constants of liquid silicon much above the melting point. Since the flat portion τ_m of the reflectivity curve corresponds to the characteristic time duration of melt, variation of this time with respect to laser fluence was also studied. The results are depicted in figure 8c. A good agreement was observed between theoretically calculated duration of melt and experimental results. All these results were in favour of the thermal model. Interestingly enough, however, Raman and transmission measurements carried out by Lo and Campon (1980) revealed results supporting the non-thermal model. The Stokes–anti-Stokes line ratios observed in these experiments showed unequivocally that the lattice temperature rise is far less than that necessary to melt silicon.

With the advent of basic research work such as those described above, the method of laser annealing facilitated investigations of new processing technologies for silicon integrated circuits. In the following paragraphs we have highlighted some of these novel features and applications of silicon crystal growth and solidification by the laser annealing technique.

One of the most important results of research into transient thermal processing is the technology for forming crystalline silicon on amorphous substrates. The use of conventional methods, involving chemical vapour deposition, for the synthesis of polycrystalline silicon on SiO_2 are known to yield fine grain size of 500 Å and as such its electrical transport properties are much poorer than those of single-crystal silicon. By scanning a continuous laser spot over such a small grain polycrystalline
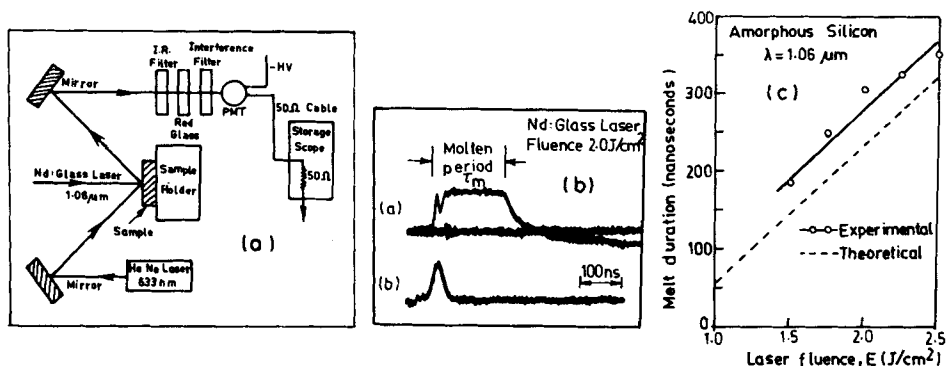

Figure 8. (a) Experimental set-up for time-dependent optical reflectivity measurements using a He–Ne laser during irradiation of self-ion-implanted amorphized silicon with a Q-switched Nd–glass laser. (b) Reflectivity profile of the Si substrate at 633 nm as it passes through the phase transitions for a laser fluence of 2·0 J/cm². Also shown is 50 ns laser pulse. (c) Theoretical and experimental values for melt duration versus laser fluence during laser irradiation of self-ion-implanted amorphized silicon with a Q-switched Nd–glass laser (50 ns FWHM). (Bhattacharyya *et al* 1981.)

film a major increase in grain size could be achieved (figure 9a). This method requires a laser intensity high enough to produce a region of molten silicon. The silicon recrystallizes in the trailing edge of this molten spot. This type of crystallization is called lateral crystal growth or lateral epitaxy (Gat *et al* 1978). Such a recrystallized material is still not ideal for device purposes, although it compares quite favourably with the best known "silicon-on-insulator material" and epitaxial silicon on sapphire. With a view to further increase the grain size in laterally grown silicon, Biegelsen *et al* (1981) studied the effect of "shape of laser spot during annealing" on crystallization. With the technique suggested by them, crystal islands as wide as 20 microns could be grown. The overall success of lateral crystal growth led them to construct novel two-level, high-rise c-mos devices. In contrast to laser-induced crystallization, laser-induced amorphization has also been observed under appropriate conditions of processing. When quench rates or regrowth velocities are fast enough precipitation of amorphous silicon occurs. The first of these important observations was made by Liu *et al* (1979) and Tsu *et al* (1979) when they used picosecond pulses of ultraviolet light. The calculations indicate that the velocities required for such a phenomenon are in the vicinity of 20 m/sec. Researchers have also tried to control the crystal orientation during laser annealing. They used an underlying crystalline substrate in conjunction with the scanning beam technique to direct or "seed" the crystal orientation of solidifying surface layer (figure 9b). Al Tasch and his associates report seeding crystal growth to distances of 30 microns over SiO_2 substrate. Several such studies have been carried out exploring the use of laser annealing in device fabrication.

The most common application of pulsed lasers has been in the context of photo-voltaics, viz. formation of p–n junctions in silicon solar cells. Different approaches have been reported for the use of laser processing for junction formation (Wood *et al* 1980).

The effect of laser annealing on ion-implanted layers is well established. The conventional thermal annealing method is of limited use in achieving full activation of implanted dopants particularly in the case of high-dose implants. Laser annealing
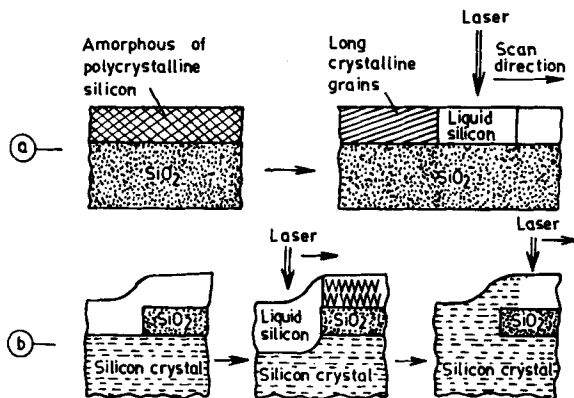

Figure 9. Lateral epitaxy. Schematic diagrams show two methods by which a continuous laser can produce a thin layer of single-crystal silicon on a silica substrate. **(a)** Without seeding. **(b)** With seeding. An opening in the silica layer puts the molten silicon in contact with a silicon crystal, which defines the crystal orientation of the solidifying liquid. (Poate and Brown 1982.)

was found to be useful in such situations. Figure 10 shows the carrier concentration as a function of implanted dose for a series of boron-implanted Si samples. It is clear from the figure that at higher doses full activation of implanted dopants can be achieved by using laser annealing, although it is not possible by using the conventional thermal annealing method. Figure 11 shows quantum efficiency curves for different B^+-implanted cells. It is clear from these results that the laser-annealed solar cell has better spectral response than a single-step thermally annealed cell. In this case more sophisticated multi-step thermal annealing can further improve the quantum response significantly but it adds to the complexity of the processing. In the case of laser-annealed samples the quantum response of the 5 keV implanted cell is better than that of the 35 keV implanted cell. It should also be noted that the minority carrier diffusion length in the base region (given by L in the figure) is much greater for the laser-annealed 35 keV implanted samples than it is for the
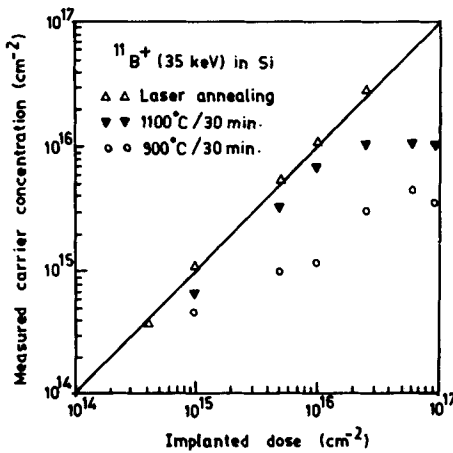

Figure 10. Carrier concentration as a function of implanted dose in thermally annealed and laser annealed samples. (Wood *et al* 1980.)
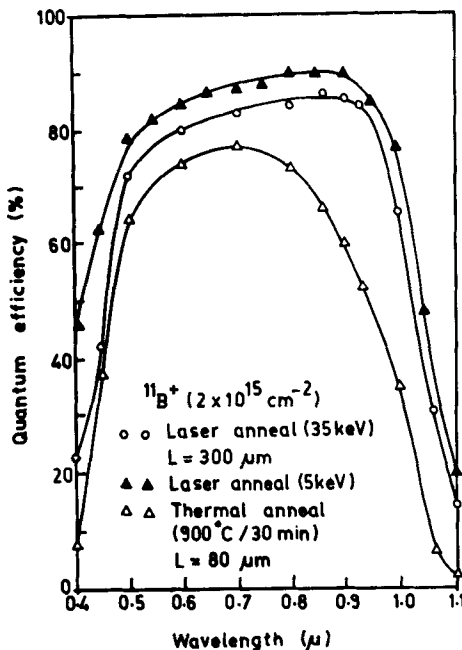

Figure 11. Spectral response of three B-implanted solar cells. L is the minority carrier diffusion length in the base region. (Wood *et al* 1980.)

thermally annealed sample. Preservation of the minority carrier diffusion length is characteristic of laser processing and occurs because the temperature in the base region of the sample is never raised significantly above the ambient temperature.

Another method of introducing dopant into near-surface region is the laser-induced diffusion of surface-deposited dopants. This approach relies on the fact that thin films (a few tens of Angstroms) of dopants, e.g. B and Al, deposited on Si substrate can be driven into the sample as a consequence of liquid-state diffusion during laser-induced melting of near-surface region. Transmission electron microscopy and electrical measurements show that the dopants are dissolved in the Si lattice and are electrically activated. The results of I–V and reversed biased C–V measurements indicate that defect-free junctions can be obtained by this method and the efficiencies of solar cells made by this method are generally found to be comparable to those of the ion-implanted, laser-annealed cells. The technique is particularly attractive for terrestrial solar cell applications because it seems that appropriate junctions can be formed by using low-cost deposition techniques such as chemical spraying, dipping, etc. which bypass the expensive ion implantation and high-temperature furnace processing completely. Recently it was shown that the doped layers of a-Si (a few hundred Angstroms thick) can also be transformed into an active junction by using laser processing.

In addition to synthesizing active regions, a number of other applications of pulsed lasers in device processing are being explored. Since this is an optical processing method, with an appropriate focusing mechanism it can be easily rendered highly area-selective. Thus, with an appropriate choice of parameters, processing of near-surface layers can be done without affecting the pre-synthesized region below the surface layers of solid. An example is the synthesis of silicon dioxide layers. The conventional method of preparation of SiO_2 films involves processing at elevated temperatures (1000°C) and as such this is detrimental to the pre-synthesized silicon. Blum *et al* (1983) have reported the use of laser treatment in such situations. These studies revealed that silicon monoxide films can be converted to silicon dioxide by excimer laser treatment. Since SiO films can be vapour-deposited on the substrate at room temperature, subsequent laser treatment would result in formation of SiO_2.

Finally, we would like to concern ourselves with an interesting phenomenon, viz. "explosive crystallization", observed in the context of pulsed laser annealing of a-Si. This phenomenon basically refers to the existence of self-propagating melt-front in a direction opposite to that of regrowth of laser-induced molten layers. The reasons for expecting such an effect are based on the fact that a-Si has higher free energy than c-Si (Bagley *et al* 1979). The free energy curves for a-Si, c-Si and molten silicon revealed that the amorphous phase would melt at considerably lower temperature (T_a) than the crystalline phase (T_c). The results of an experiment carried out by Sinke *et al* (1984) support this proposition. The experiment was basically in the context of low-energy laser irradiation of Cu-implanted silicon. In these studies Cu was implanted in c-Si to yield an amorphous surface layer of thickness 225 nm. These samples were subsequently laser-treated by using 20 ns ruby laser, with various energy densities ranging between 0·1 and 2·0 J/cm². Since Cu diffuses much faster in liquid silicon than in solid silicon, strong surface segregation effects were expected, in view of melting and rapid regrowth of surface layers after laser treatment. The amount of surface segregation should have been dependent upon laser beam energy which defines the primary melt depth from the

surface of the silicon sample. In addition to surface segregation, however, strong segregation effects were also observed at depths much greater than the depth of primary melt. Figure 12 shows variation of implanted Cu profiles after laser irradiation at different energy densities. It is clear that for energy densities greater than $0.2 \, \text{J/cm}^2$ there is the appearance of a double-peak structure in the concentration profile of Cu indicating segregation effects. To explain these additional segregation effects, it is argued that, subsequent to initial melting, there exist two resolidification fronts. One front is the conventional liquid–solid interface coming towards the surface of the sample while the other front, viz. secondary melt-front, goes towards the interface of c-Si–a-Si. The existence of secondary melt-front was explained on the basis of the difference in melting point of amorphous and crystalline silicon. Thus, when crystallization of laser-induced molten layers begins, it will lead to release of latent heat (H_c). Since 'H_c' is larger than the heat needed to melt the equivalent amount of a-Si (H_a), the released energy may be used to melt the underlying a-Si layer. Again during crystallization of this secondary melted silicon layer, energy may be released and subsequently utilized to melt the next layer of a-Si. If this process proceeds, it would result in a self-propagating layer of melted silicon moving from the surface region towards the a-Si–c-Si interface. From the direction in which this secondary melt-front moves it is clear that it will lead to a segregation of copper towards a-Si–c-Si interface. Depending upon the temperature gradient in the a-Si layer, this explosive crystallization may either quench at a certain depth or proceed through the entire amorphous layer.
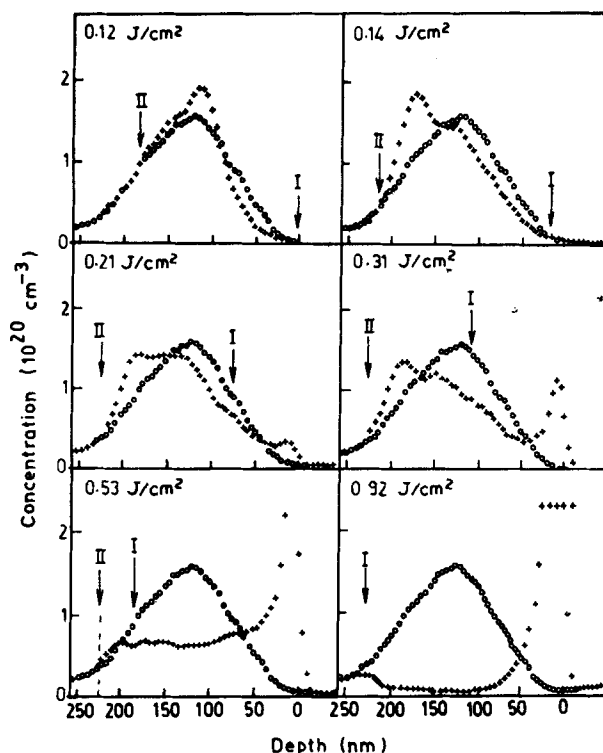

Figure 12. The 'Cu' concentration profile in Cu-implanted silicon, before (circles) and after (crosses) pulsed laser irradiation at various energy densities. Indicated are primary (I) and secondary (II) melt depths. (Sinke and Saris 1984).

In this article we have discussed many aspects of rapid crystal growth and solidification effects in silicon induced by pulsed laser treatment. It is clear that though much work has been done in this field, many features of laser-induced phenomena still remain to be explored, thus making it an exciting area of research.

Acknowledgements

References

Bagley B G and Chen H S 1979 *in Laser-Solid Interaction and Laser Processing—1978* (eds) S D Ferris, H J Leamy and J M Poate, *AIP Conf. Proc. No.* 50, p. 97

Baeri P, Compisano S V, Foti G and Rimini E 1978 *Phys. Rev. Lett.* **41** 1246

Baeri P, Compisano S V, Foti G and Rimini E 1979 *J. Appl. Phys.* **50** 788

Baeri P, Foti G, Poate J M, Campisano S V and Cullis A G 1981 *Appl. Phys. Lett.* **38** 800

Bhattacharyya A, Streetman B G and Hess K 1981 *J. Appl. Phys.* **52** 3611

Biegelsen D K, Johnson N M, Bartelink D J and Moyer M D 1981 *in Laser and electron beam solid interactions and material processing.* (eds) J F Gibons, L D Hess, T W Sigmon Vol 1, *Met. Res. Soc. Symp. Proc.* (New York: North Holland) p 487

Blum S E, Brown K H and Shrinivasan R 1983 *Appl. Phys. Lett.* **43** 1026

Cahn J W, Coriell S R and Boetinger W J 1980 *in Laser and Electron beam processing of materials* (eds) C W White and P S Peercy (New York: Academic Press) p 89

Cole J M, Humphreys P and Earwaker L G 1984 *Vacuum* **34** 871

Gat A, Gerzberg L, Gibbons J F, Magee T J, Peng J and Hong J D 1978 *Appl. Phys. Lett.* **33** 775

Gelvin G L, Thompson M O, Mayer J W, Hammond R V and Percy P S 1982 *Phys. Rev. Lett.* **48** 33

Gerasimenko N N, Dvurechensky A V, Kuchurin G N, Pridachin N B and Smirnov L S 1975 *Proc. Int. Conf. Ion Implantation, Budapest*

Khaibulin I B, Titov V V, Shtyrkov E I, Zaripov M M, Stashko V P and Kuzmin K P 1975 *Proc. Int. Conf. Ion Implantation, Budapest*

Hoonhout D and Saris F W 1979 *Phys. Lett.* **A74** 253

Hoonhout D, de Jong T and Saris F W 1980 *J. de. Physique.* **C4** 89

Hoonhout D 1981 Ph.D thesis. FOM Inst. of Atomic and Molecular Physics, Amsterdam, The Netherlands

Liu P L, Yen R, Bloembergen N and Hodgson R T 1979 *Appl. Phys. Lett.* **34** 864

Liu J M, Yen R, Kurz H and Bloembergen N 1982 *Appl. Phys. Lett.* **39** 755

Lo H W and Campon A 1980 *Phys. Rev. Lett.* **44** 1604

Narayan J 1981 *J. Appl. Phys.* **52** 1289

Poate J M 1982 *in laser and electron beam interaction with solids* (eds) B R Appleton and G K Celler Vol 4, *Mater. Res. Soc. Symp. Proc.* (New York: North Holland)

Poate J M and Brown W L 1982 *Physics Today* **24**

Prussin S and Wan-der Ohe W 1980 *J. Appl. Phys.* **51** 3853

Shtyrkov E I, Khaibulin I B, Zaripov M M, Galyatudinov M F and Bayazitov R M 1975 *Proc. Int. Conf. Ion Implantation, Budapest*

Sinke W and Saris F W 1984 *PRL* **53** 2121

Spaepen F and Turnbull D 1979 In *Laser-Solid Interaction and Laser Processing—1978* (eds) S D Ferris, H J Leamy and J M Poate, *AIP Conf. Proc. No.* 50, p. 73

Tamminga Y, Eggermont G E J, Hofker W K, Hoonhout D, Gerrelt R and Saris F W 1979 *Phys. Lett.* **69A** 436

Tsu R, Hidgson R T, Tan Y A and Baglin J E E 1979 *Phys. Rev. Lett.* **42** 1356

White C W, Wilson S R, Appleton B R and Young Jr. F W 1980 *J. Appl. Phys.* **51** 738

White C W *et al* 1978 *Proc. Int. Conf. on Ion beam modification of materials, Budapest*

Wood R F, Kirkpatrick J R and Giles G E 1981 *Phys. Rev.* **B23** 5555

Wood R F and Young R T 1980 *IEEE Vol* p 688